Science of the Total Environment 931 (2024) 172507

Contents lists available at ScienceDirect

Science of the Total Environment

journal homepage: www.elsevier.com/locate/scitotenv

Metagenomes from microbial populations beneath a chromium waste tip give insight into the mechanism of Cr (VI) reduction

Douglas I. Stewart [a,*], Elton J.R. Vasconcelos [b], Ian T. Burke [c], Alison Baker [d]

[a] School of Civil Engineering, University of Leeds, Leeds LS2 9JT, UK
[b] Leeds Omics, University of Leeds, Leeds LS2 9JT, UK
[c] School of Earth and Environment, University of Leeds, Leeds LS2 9JT, UK
[d] School of Molecular and Cellular Biology, University of Leeds, Leeds LS2 9JT, UK

HIGHLIGHTS

- Cr(VI) leaching from COPR waste sites into ground water is a threat to health.
- The capacity of in situ soil microbial populations to reduce Cr(VI) was studied.
- Microcosms spiked with Cr were analysed by geochemical and molecular methods.
- A unique microbial population reduced Cr via acetate stimulated sulfate reduction.
- In situ microbial populations have the potential to remediate COPR legacy sites.

GRAPHICAL ABSTRACT

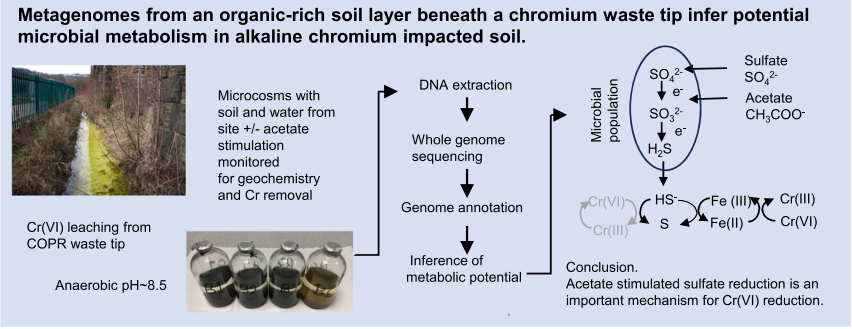

ARTICLE INFO

Editor: Christopher Rensing

Keywords:
COPR
Acetate
Anaerobic sulfite reduction
Dissimilatory sulfate reduction
Whole genome sequencing
Alkaline environment

ABSTRACT

Dumped Chromium Ore Processing Residue (COPR) at legacy sites poses a threat to health through leaching of toxic Cr(VI) into groundwater. Previous work implicates microbial activity in reducing Cr(VI) to less mobile and toxic Cr(III), but the mechanism has not been explored. To address this question a combined metagenomic and geochemical study was undertaken. Soil samples from below the COPR waste were used to establish anaerobic microcosms which were challenged with Cr(VI), with or without acetate as an electron donor, and incubated for 70 days. Cr was rapidly reduced in both systems, which also reduced nitrate, nitrite then sulfate, but this sequence was accelerated in the acetate amended microcosms. 16S rRNA gene sequencing revealed that the original soil sample was diverse but both microcosm systems became less diverse by the end of the experiment. A high proportion of 16S rRNA gene reads and metagenome-assembled genomes (MAGs) with high completeness could not be taxonomically classified, highlighting the distinctiveness of these alkaline Cr impacted systems.

Abbreviations: AnSR, anaerobic sulfite reduction; APS, Adenosine 5'-Phosphosulfate; ATP, Adenosine triphosphate; BC, Bray-Curtis beta diversity value; COPR, Chromium Ore Processing Residue; DSR, dissimilatory sulfate reduction; KEGG, Kyoto Encyclopaedia of Genes and Genomes; LOI, Loss on Ignition; MAG(s), Metagenome Assembled Genome(s); NADH, Nicotinamide Adenine Dinucleotide + Hydrogen; OTU(s), operational taxonomic unit(s); qXRD, quantitative x-ray diffraction analysis; RIR, Relative Intensity Ratio; rRNA, ribosomal Ribonucleic Acid; SOM, Soil Organic Matter; WGS, Whole Genome Sequencing; XRF, X-ray Fluorescence.

* Corresponding author.
E-mail addresses: d.i.stewart@leeds.ac.uk (D.I. Stewart), E.Vasconcelos@leeds.ac.uk (E.J.R. Vasconcelos), i.t.burke@leeds.ac.uk (I.T. Burke), a.baker@leeds.ac.uk (A. Baker).

https://doi.org/10.1016/j.scitotenv.2024.172507
Received 28 October 2023; Received in revised form 4 April 2024; Accepted 13 April 2024
Available online 23 April 2024

Examination of the coding capacity revealed widespread capability for metal tolerance and Fe uptake and storage, and both populations possessed metabolic capability to degrade a wide range of organic molecules. The relative abundance of genes for fatty acid degradation was 4× higher in the unamended compared to the acetate amended system, whereas the capacity for dissimilatory sulfate metabolism was 3× higher in the acetate amended system. We demonstrate that naturally occurring in situ bacterial populations have the metabolic capability to couple acetate oxidation to sequential reduction of electron acceptors which can reduce Cr(VI) to less mobile and toxic Cr(III), and that microbially produced sulfide may be important in reductive precipitation of chromate. This capability could be harnessed to create a Cr(VI) trap-zone beneath COPR tips without the need to disturb the waste.

1. Background

Chromium chemicals are used in many industrial processes (Barnhart, 1997; Jacobs and Testa, 2005; ENTEC, 2008). Chromium has two environmentally stable oxidation states: Cr(III) and Cr(VI) (Pourbaix, 1966; Brito et al., 1997). It is extracted from chromite ore by heating with an alkali-carbonate to 1150 °C to oxidise insoluble Cr(III) to soluble Cr(VI), which is then extracted with water upon cooling. Originally, limestone was added to the reaction to improve air penetration (Breeze, 1973; Darrie, 2001). This "high-lime" process was superseded by lime-free processing in about 1960 (Alderson and Rattan, 1981), but the simplicity of the process meant it continued to be widely used until the end of the 20th Century, particularly where environmental regulations were less stringent (Darrie, 2001). Some of the most intractable environmental problems from chromium contamination of soil and groundwater are associated with poor disposal of chromite ore processing residue (COPR) from the high-lime process. Lack of regulation or enforcement at the time when these wastes were produced means that water ingress and subsequent leaching poses a threat to groundwater, as water in contact with high-lime COPR can have a pH > 12 and contain up to 80,000 μg/L Cr(VI) (Whittleston et al., 2011b).

Cr(III) is an essential trace element for mammals (Lukaski, 1999; Vincent, 2000; Cefalu and Hu, 2004). In contrast, Cr(VI) is toxic to plants, animals and humans (Costa, 1997; Chandra and Kulshreshtha, 2004; Shanker et al., 2005) and is classified as a mutagenic and carcinogenic material (Léonard and Lauwerys, 1980; Kondo et al., 2003). Concern about the long-term health impacts of Cr(VI) ingestion have led to the World Health Organisation to recommend a maximum of 50 μg/L total chromium in drinking water, and the California Water Resources Control Board to set a maximum contaminant level of 10 μg/L Cr(VI) for drinking water (WHO, 2020; SWRCB, 2022).

Water in equilibrium with COPR can contain up to 80,000 μg/L Cr (VI), however, at several disposal sites where COPR leachate has fortuitously seeped into organic matter-rich soils, chromium has accumulated in its reduced Cr(III) form associated with Fe(III) oxyhydroxides after reaction with microbially reduced iron (Burke et al., 1991; Whittleston et al., 2011b; Ding et al., 2016). Recent developments in whole genome sequencing and the associated bioinformatic analyses have opened up the possibility to catalogue the metabolic capabilities of microbial populations in environmental samples. Since many microorganisms are unknown and unculturable (Albertsen et al., 2013), these methods allow insights into the structure and metabolic potential of microbial communities, which are impossible to obtain by culture based methods. Contaminated sites present an extreme environment for life with multiple stressors; in the case of COPR disposal sites the combination of toxic metals and alkaline pH. Probing the microbial communities of such extreme environments can reveal the biochemical potential, which could be harnessed for remediation processes. While metagenomics has been applied to several alkaline environments, often saline lakes and/or hot springs (Vavourakis et al., 2018; Cotta et al., 2022) and alkaline sulphidic mine tailings (Bier et al., 2020; Li and Li, 2021), this is the first time it has been used at a COPR disposal site.

The aim of our study was to explore the microbial community in the soil layer under a historical COPR waste pile and examine how it evolved and responded in anaerobic microcosms with and without acetate stimulation (addition of an organic electron donor, such as acetate, can increase the rate of microbial metabolism in systems where natural organic matter is low in concentration or unreactive; Lovley, 1993). Complementary geochemical data was collected to provide context and to allow the changes in microbial diversity and metabolic capability to be related to changes in availability of key chemical species relevant to Cr speciation and mobility. Metagenomes from these alkaline, Cr contaminated soils were analysed for genes for stress resistance and metabolic capabilities. This information will help to understand how microbial populations interact with the geochemistry at waste sites and how potentially this could be managed to reduce Cr(VI) leaching.

2. Methods

2.1. Site description

The study site was a 19th century COPR tip covering an area of 1.8 ha is located in a river valley in the North of England (Fig. 1a: Stewart et al., 2010). The waste was tipped against the valley side between a canal and the river which are about 150 m apart; the canal follows the valley side and is about 7 m higher than the river; Fig. 1b. Ground level on the tip is about 1.5 m higher than the canal towpath. Geological maps indicate that this is a glacial valley within the millstone grit series that has been partially in-filled with alluvial deposits (silt, clay and sand). Prior ground investigations of the tip have revealed that the COPR waste was placed directly onto the alluvial soils and then covered with topsoil (Whittleston et al., 2011a). Beneath the tip is a thin soil layer, described as a grey clay, which is rich in soil organic matter and thought to have been the surface layer prior to COPR tipping. This is underlain by alluvial sand and gravel with some cobbles of sandstone. A confidential commercial site investigation undertaken in 2007 indicated that the alluvial deposits are ~8 m thick. A hydrogeology study in April 2009 (Atkins, 2009) showed a perched water table within the waste just over 2 m above the water table in the underlying alluvial deposits, and that flow in the alluvial deposits is roughly south-westerly from the valley side towards the river (roughly along the cross-section in Fig. 1). This indicates that water from the COPR tip initially flows downward and then towards the river. Chromium has accumulated in grey clay, exclusively in its reduced Cr(III) form associated with Fe(III) oxyhydroxides (Whittleston et al., 2011b).

2.2. Soil sampling

Soil samples were collected in June 2021 from a borehole that was advanced through the side-slope on western corner of the waste tip using a hand auger and 1 m core sampler (Fig. 1). This borehole revealed 1.8 m of compacted topsoil, over 1.1 m of COPR waste, over grey clay soil. Three samples of the grey clay were recovered from depths of 2.9 m, 3.4 m and 3.6 m (0 m, 0.5 m and 0.7 m below the COPR). A water sample was taken from the site drainage ditch close to where it enters the river (at the base of the viaduct; Fig. 1). Soil samples were double-bagged in sealed polythene bags and stored at 4 °C in the dark in an oxygen-free atmosphere using Anaerogen™ sachets. Water samples were stored at

4 °C in completely full sealed polythene containers. Experiments were started within 2 days of collecting the samples. A sample of the grey clay from a depth of 3.4 m (the original soil) was frozen for DNA extraction and 16S rRNA gene sequencing.

2.3. Microcosm experiments

Microcosms were made from 10 g of clay from a depth of 3.4 m (0.5 m below the COPR) and 100 mL of ditch water in 120 mL Wheaton glass serum bottles. These were purged with N_2 and sealed with butyl rubber stoppers and aluminium crimp-seals (Merck Life Sciences, Germany). Triplicate *active* microcosms and a *sterile* control microcosm were prepared for two systems. There were no further additions to the "*unamended*" system. Sodium acetate to a final concentration of 20 mmol. L^{-1} was added to "*Acetate amended*" system (acetate at this concentration has previously been shown to support microbial metabolism in reduction microcosm experiments without being exhausted over periods exceeding 2 months; Stewart et al., 2007). Controls were prepared by autoclaving soil in bottles with a N_2 purged headspace soil (121 °C for 15 min) before injecting filter sterilised ditch water upon cooling. All microcosms and controls were incubated anaerobically at 21 ± 2 °C in the dark. The microcosms were allowed to establish for 5 days, before they were spiked with K_2CrO_4 to a final concentration of 500 μmol.L^{-1} Cr(VI), run for a further 64 days, spiked again with K_2CrO_4 at the same concentration (day 69), before the microbiology was sampled on day 71.

Microcosms were periodically sub-sampled for geochemical analysis. During sampling the bottles were shaken and 3 mL of soil slurry withdrawn through the stopper using aseptic technique with sterile syringes and needles (Burke et al., 2006). Samples were centrifuged (5 min, 16,000 g) and the pore water and soil were analysed.

2.4. Geochemical methods

Aqueous Cr(VI) was determined by standardised UV–vis spectroscopy methods on a Shimadzu UV-1900 (US-EPA, 1992). Standards were used regularly and calibration linear regressions normally produced r^2 values >0.99. Chloride, nitrite, nitrate and sulfate were determined by ion chromatography on a ThermoScientific ICS5000 with AS19 and AG19 analytical columns. Acetate concentration was determined by repeat IC analysis with the eluent concentration optimised for that analyte. As a proxy for microbial available Fe (Weber et al., 2001; Burke et al., 2006), the percentage Fe(II) in the soil was determined after extraction by 0.5 N HCl and reaction with ferrozine (Lovley and Phillips, 1986). pH was determined using Denver Instruments UB-10 bench-top meter and Sentek P11 pH electrode calibrated at 7 and 10, daily.

Loss on ignition (LOI) at 550 °C (4 h) was determined on samples that were first oven dried at 105 °C (24 h). Relative Intensity Ratio (RIR) quantitative x-ray diffraction analysis (qXRD) was carried out on the Bruker D8 XRD. Samples were initially ground to <75 μm using a Retsch RS200 disc mill, before being combined with 20 % corundum and ground again in a 5%PVA solution using a McCrone microniser. The slurry was spray dried onto a slide to produce randomly orientated particles, and samples were scanned between 2 and 70° 2θ using Cu $K\alpha_1$ radiation. Trace elements (Fe, S and Cr) in the clay samples were

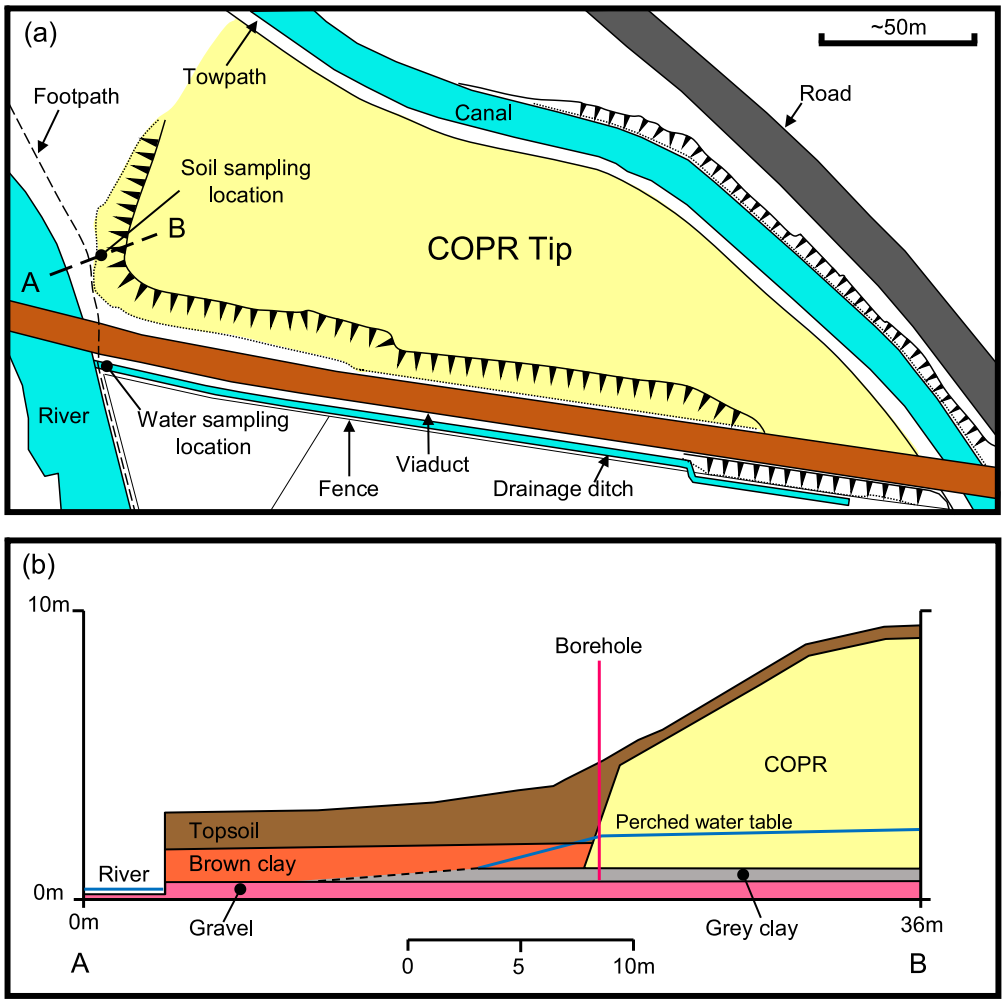

Fig. 1. (a) Sketch map of the site showing the borehole location, and (b) conceptual ground model along the line AB.

determined using an Olympus Innovex X-5000 energy dispersive X-ray Fluorescence spectrometer (XRF).

2.5. Microbiological methods

Microbial genomic DNA was extracted from subsamples (~0.25 g) using a DNeasy PowerSoil Kit (QIAGEN Ltd). DNA concentration was quantified using a Qubit™ dsDNA HS Assay Kit on a Qubit® 2.0 Fluorometer (Invitrogen) and concentrations were from 4 to 30 ng/μl. DNA samples were sent to the Next Generation Sequencing Facility at the Leeds Institute for Biomedical and Clinical Sciences for 16S rRNA gene sequencing targeting the hyper-variable V4 region (MiSeq - 250 bp paired-end reads, 400 k reads per replicate) and whole genome sequencing (NextSeq 2000–150 bp paired-end reads, 100 M reads per system).

2.6. 16S rRNA gene microbiome data analysis

Software and algorithms used for 16S rRNA gene and metagenomics analysis are listed in SI Table S1.

UPARSE pipeline (Edgar, 2013) was used for the 16S rRNA gene-NGS data analysis, setting a 97 % identity threshold for clustering operational taxonomic units (OTUs). Sufficient reads were recovered from all soil samples to randomly select 18 k reads per soil sample after quality control for subsequent analysis. Taxonomic classification of OTUs was undertaken using the RDP 16S rRNA training database version 16 (Cole et al., 2014) using a confidence value of 0.7 to give a reasonable trade-off between sensitivity and error rate in the taxonomy prediction. OTUs which were not classified as bacteria with a confidence >0.7 (e.g. Archaea and poor reads) were not included in the diversity and statistical analyses. Hill numbers (D_q) were used to characterise bacterial diversity in the samples (Hill, 1973), where D_0 is the OTU richness, and D_1 and D_2 are measures of the number of common and dominant OTUs. Bray-Curtis beta diversity values were used to characterise dissimilarity between the replicates.

2.7. Metagenomics data analyses

An ad-hoc establishment of the MetaWRAP pipeline (Uritskiy et al., 2018) was deployed to run the metagenomics data analysis workflow. Quality control was assessed through both FastQC (Babraham_Bioinformatics, 2023a) and multiQC (Ewels et al., 2016), whereas trimming of low quality bases (QV < 20) and adapters was performed by TrimGalore (Babraham_Bioinformatics, 2023b). WGS data from the biological triplicates from each system (unamended and acetate amended) had their trimmed fastq files concatenated (pooled) for the initial assembly process with metaspades (Nurk et al., 2017): –checkpoints last –only-assembler −1 $reads_1–2 $reads_2. Metaspades-generated contigs were then submitted to the metaWRAP binning module that makes use of three independent algorithms: CONCOCT (Alneberg et al., 2014), MetaBat2 (Kang et al., 2019), and MaxBin2 (Wu et al., 2016). The three binning sets were refined through the "bin_refinement.sh" module that used CheckM (Parks et al., 2015) for quality assessment and initial taxonomic classification survey of all assembled bins, setting a cutoff of 90 % completeness (−c 90) and 10 % contamination (−x 10). Bins' reassembly was performed by SPAdes (Prjibelski et al., 2020) with default parameters through the "reassemble_bins.sh" module. The last two modules (classify_bins and annotate_bins) relied on Taxator-tk (Dröge et al., 2015) and Prokka (Seemann, 2014) for a final taxonomic classification of each metagenome-assembled genome (MAG) and gene functional annotation, respectively. The prefix A was added to labels for MAGs from the unamended system and the prefix B was added to labels for MAGs from the acetate amended system. Both prokka2kegg python script (SilentGene, 2019) and MinPath algorithm (Ye and Doak, 2009) were added at the end of the metaWRAP annotate_bins module execution. Prokka2kegg maps KEGG pathways to the gene IDs of the MAGs to determine KEGG orthologs (KOs) (Aoki-Kinoshita and Kanehisa, 2007). MinPath uses a parsimony approach to reconstruct biological pathways to provide a conservative estimation of the metabolic pathways within a MAG and assign a boolean significance score (Ye and Doak, 2009). This ad-hoc deployment in the pipeline allowed us to properly assess metabolic pathways in each sample group. All other metaWRAP intermediate/optional modules were run using its default parameters.

The functional annotation files for the MAGs that were > 90 % complete were searched for genes coding for resistance to various metal (loid)s (Table S2). Each individual sample group also had their final metaWRAP-generated MAGs' fasta files used as input for FeGenie (Garber et al., 2020) (−-meta –norm –heme –hematite –makeplots), in order to assess for enrichment of iron metabolism-related genes. Sequence conservation was assessed through megaBLAST (Altschul et al., 1997), where MAGs from the unamended system (A) were compared pairwise with MAGs from the acetate amended system (B). Contigs from the first MAG were aligned to contigs from the second, and the proportion of the first MAG, for which there was a reliable match (>80 % identity over >50 % alignment coverage, and e-value <0.001), was calculated to identify potential pairs. MAGs' pairings where the sum of contigs' alignment lengths was less than one third of the whole MAG length were disregarded. It resulted in nineteen MAGs from the unamended system (A) that reliably matched to MAGs from the acetate amended system (B), displaying sequence conservation across over 33 % of its whole length.

ZicoSeq R package (Yang and Chen, 2022) was employed for differential abundance analysis of MAGs from systems A versus B, relying on GCPM (genome copies per million reads) quantification values generated after the quant_bins module execution in the metaWRAP pipeline. A *p*-value threshold of 0.01 was set on ZicoSeq's output.

The functional gene annotation files of all the MAGs from both systems were searched for the genes required for dissimilatory sulfate reduction (DSR) and anaerobic sulfite reduction (AnSR), by name, synonyms, and their KEGG Orthology numbers. The search terms and synonyms are given in SI Table S3. For MAGs containing at least 1 of these diagnostic genes, we relied on MinPath (Ye and Doak, 2009) output tables to determine the number of genes associated with a significant (MinPath positive) sulfur metabolism KEGG pathway (00920) assignment. This allowed generation of two DSR 2 × 2 contingency tables for each MAG: involved in DSR/AnSR (row 1), not involved in DSR/AnSR (row2), in the MAG (col 1), and not in the MAG (col 2). Then, a Fisher Exact Test was used to determine whether the proportion of DSR and AnSR genes were significantly greater than the proportion of sulfur metabolism genes found (p-value <0.05).

A heat map of DSR and AnSR genes' abundance across all MAGs from both systems that contained them was plotted through the *pheatmap* R package (Kolde, 2019). For the colour shading, we considered as abundance (A) the number of gene copies in the gene set (columns) per MAG (rows) times the MAG's GCPM. A hierarchical clustering relying on $Log_2(A + 1)$ values was performed for both rows and columns prior to plotting.

RCircos (Zhang et al., 2013) was employed for summarising DSR and AnSR gene loci on the most abundant MAGs through a circosPlot. The same abundance (A) metric established for the heat map was used for creating an "abundance inner track" in the plot. In addition, a tBlastX (Altschul et al., 1997) pairwise analysis was performed between the plotted MAGs in order to identify amino acid sequence conservation in different stretches along different MAGs (coloured linking lines in the middle of the circosPlot). We set e-value $<1e^{-3}$, alignment length ≥ 90 nt (or 30 aa), and identity ≥50 % as threshold for tBlastX outputs.

3. Results

The three samples of grey clay had a similar mineralogical composition; predominantly quartz with illite/smectite, some albite and

smaller amounts of mica and kaolinite (SI Table S4). Clay minerals formed a total of about 30 % of each sample. The grey clay used in the microcosms contained 4.0 wt% Fe, 0.3 wt% S, and 0.3 wt% Cr (SI Table S5). LOI was 7.9 wt% suggesting it contained about 3 wt% soil organic carbon, SOC (Jensen et al., 2018). The ditch water had a pH value of 8.9 and contained 115 μmol.L^{-1} (6000 μg/L) Cr(VI) (see SI Table S6 for composition).

3.1. Microcosm experiments

The microcosms were first sampled ~90 min after establishment. At this point the geochemistry of the two systems was very similar (Fig. 2 and SI Fig. S1). The initial pH of the unamended microcosms was 8.8 ± 0.3, and did not vary much over the experiment (SI Fig. S1(a)). The water initially contained 4.5 ± 0.6 μmol.L^{-1} Cr(VI), 140 ± 14 μmol.L^{-1} NO_3^-, and 2440 ± 210 μmol.L^{-1} SO_4^{2-}. Approximately 97 ± 3 % of the 0.5 N HCl extractable iron associated with the soil was Fe(II). The initial pH of the acetate-amended microcosms was 8.5 ± 0.1, but increased to 9.1 ± 0.1 over the experiment. The water initially contained 8.9 ± 5.6 μmol.L^{-1} Cr(VI), 123 ± 3 μmol.L^{-1} NO_3^-, and 2020 ± 210 μmol.L^{-1} SO_4^{2-}. Approximately 88 ± 9 % of the acid extractable iron was initially Fe(II), but this increased steadily to 97 ± 5 % by day 6.

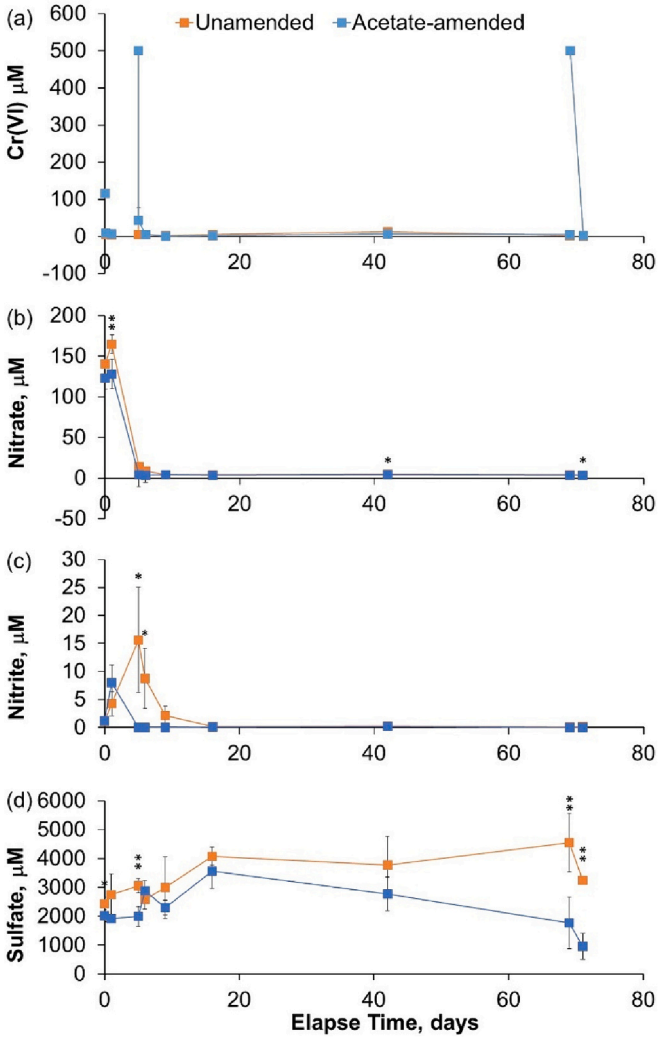

Fig. 2. Geochemical conditions in the unamended and acetate-amended microcosms (a) Cr(VI) concentration, (b) nitrate concentration, (c) nitrite concentration and (d) sulfate concentration. Error bars represent one standard deviation of triplicates. Annotation indicates a significant difference between the two systems at the same time point (Student's *t*-test:$^{*}_{*}$ $p \leq 0.05$ and * $p \leq 0.10$).

All the Cr(VI) introduced with the ditch water was removed from solution over the first 24 h in both systems (Fig. 2(a)). Both subsequent Cr(VI) spikes were also removed from solution within 24 h in both microcosm series. Very little change in the proportion of the acid extractable iron that was Fe(II) was observed due to either Cr(VI) spike (SI Fig. S1(b)).

The aqueous nitrate concentration in the microcosm experiments ~90 min after establishment exceeded the amount in the ditch water by 50 to 70 % indicating that a modest amount of nitrate was released from the soil (Fig. 2(b)). However, nitrate was removed from both systems during the first few days, so that when the Cr(VI) was respiked on day 5, the unamended microcosm contained 14 ± 15 μmol.L^{-1} NO_3^-, and the acetate-amended microcosm contained 4 ± 0.5 μmol.L^{-1} NO_3^-. During this period aqueous nitrite was detected in both systems, but the concentration was higher and persisted for longer in the unamended system (Fig. 2(c)).

Despite some scatter, the sulfate concentration exhibited a modestly increasing trend in both microcosm series during the first two weeks, reaching 4080 ± 310 μmol.L^{-1} in the unamended microcosms and 3570 ± 620 μmol.L^{-1} in the acetate-amended microcosms (Fig. 2(d)). Subsequently there was little change in sulfate concentration in the unamended microcosms until day 68 after which there was a modest decrease to a final concentration of 3240 ± 80 μmol.L^{-1}. However, in the acetate-amended microcosms, there was a decrease in the sulfate concentration starting after day 15, reaching a final concentration 960 ± 450 μmol.L^{-1}. The mean acetate concentration was 16 μmol.L^{-1} in the unamended microcosms, and 20.4 mmol.L^{-1} in the acetate-amended microcosms with no systematic variation during the either experiment (SI Fig. S1(c)).

3.2. 16S rRNA gene sequence analysis

On average 77 ± 2 % (unamended), 67 ± 4 % (acetate-amended), and 77 % (original soil) of 16S rRNA gene reads were assigned to a bacterial phylum with a confidence >0.7 (see SI Fig. S2). Reads from the unamended microcosms were dominated by *Bacteroidetes* (36 ± 2 %), *Firmicutes* (21 ± 6 %), *Proteobacteria* (17 ± 4 %), and unclassified (23 ± 2 %). Reads from the acetate-amended microcosms were dominated by *Bacteroidetes* (24 ± 2 %), *Proteobacteria* (24 ± 3 %), *Firmicutes* (16 ± 2 %) and unclassified (33 ± 4 %). Whereas reads from the original soil were dominated by *Proteobacteria* (20 %), *Acidobacteria* (16 %), *Firmicutes* (14 %), *Actinobacteria* (9 %), *Chloroflexi* (6 %), *Bacteroidetes* (5 %) and unclassified (23 %).

The OTU richness (D_0^{α}), and the number of common OTUs (D_1^{α}) and dominant OTUs (D_2^{α}) were similar in the unamended (485 ± 78, 43 ± 5, 16 ± 3) and acetate amended microcosms (426 ± 85, 55 ± 9, 24 ± 3), but the diversity in both microcosms series were far lower than in the original soil ($D_0^{\alpha} = 1117$, $D_1^{\alpha} = 352$, $D_2^{\alpha} = 127$; SI Fig. S3).

Bray-Curtis beta diversity values for dissimilarity between the replicates indicate that the acetate-amended replicates were quite similar to each other at the level of OTUs (BC = 0.27, SI Table S7), whereas there was slightly more dissimilarity between the unamended replicates (BC = 0.45). There was greater dissimilarity between the unamended and acetate-amended microcosms (BC = 0.63). Both the unamended and the acetate-amended microcosms exhibited a high degree of dissimilarity from the original soil at the level of OTUs (BC = 0.92 and 0.94, respectively; Bray-Curtis values range from 0 for populations with the same composition to 1 for populations that do not share any OTUs).

3.3. Whole genome sequencing

Analysis is based on approximately 5 Gb of sequenced DNA (Phred quality score > 30) per pooled sample. All contigs generated from the first assembly step within the metaWRAP pipeline were > 1000 bp long, and about 20 % were > 5000 bp. This produced 72 and 71 MAGs from

the unamended and acetate amended microcosms, respectively. 44 MAGs from the unamended system and 32 MAGs from the acetate amended system exceeded 90 % completeness, with N_{50} values (weighted median length) for these "high quality" MAGs between 7933 and 212,796 bp, and contamination rates of 0–3.3 % and 0–3.5 %, respectively (see SI Table S8 and S9). The MegaBlast comparison of MAGs indicates that 19 MAGs in each system were very similar (see Fig. 3: any subsequent reference to one in these "paired" MAGs will include the second MAG number in brackets).

3.4. Relative abundance and identity of MAGs in the acetate-amended vs the unamended system

The proportion of the WGS reads from a system that ZicoSeq mapped onto the MAGs from that system is a guide to relative abundance of those MAGs. This indicated that *Bacteroidetes* (44 %), *Proteobacteria* (19 %) and *Firmicutes* (18 %) were the dominant phyla in the unamended system. *Proteobacteria* (38 %), *Bacteroidetes* (16 %), *Firmicutes* (6 %) were the dominant phyla in the acetate-amended system. Only 1 % of WGS reads in each system were mapped to MAGs that were classified to other phyla. This confirms the result of the 16S rRNA sequence analysis that *Bacteroidetes, Proteobacteria*, and *Firmicutes* are the most abundant phyla in both systems.

Nine MAGs from the unamended system, 11 MAGs from the acetate-amended system and 5 MAGs in each system that were paired by megaBlast were classified as *Bacteriodetes* (Fig. 3 shows the high completeness MAGs). However, the difference in the relative abundance of *Bacteroidetes* MAGs was principally due to MAG A73(B21), which were classified to the family *Flavobacteriaceae*. 32 % of WGS reads from the unamended system were mapped to A73, whereas only 2 % of reads in acetate-amended system were mapped to B21. The 16S rRNA gene analysis showed a similar result, with single OTU classified to the family *Flavobacteriaceae* accounting for the difference in relative abundance of *Bacteroidetes* reads between the two systems.

Thirteen MAGs from the unamended system, 8 MAGs from the acetate-amended system and 2 MAGs in each system that were paired by megaBlast were classified as *Proteobacteria* (Fig. 3). In the unamended system 2, 6, 3 and 2 MAGs were further classified as α-, β-, γ- and *δ-proteobacteria* (2 MAGs were not further classified), whereas in the acetate-amended system 0, 3, 0 and 7 MAGs were further classified as α-, β-, γ- and *δ-proteobacteria*. In the unamended system 11 % and 4 % of WGS reads were mapped to MAGs classified as β- and *δ-proteobacteria*, respectively, whereas 4 % and 34 % of WGS reads from acetate-amended system were mapped to MAGs that were classified to these phyla. The 16S rRNA gene analysis showed a similar difference in the relative abundance of β- and *δ-proteobacteria* in the two systems (7.4 % and 7.3 % of reads in the unamended system in comparison with 3.4 % and 20 % of reads in the acetate-amended system). Further, the only two *δ-proteobacteria* MAGs in the unamended system (A10 and A68), that were 8th and 17th most abundant MAGs in that system, were paired with the third and first most abundant MAGs in the acetate-amended system (B30 and B6, respectively). Both pairs were classified to the order *Desulfuromonadales*, and A68(B6) were further classified to the family *Geobacteraceae*.

Nine MAGs from the unamended system, 7 MAGs from the acetate-amended system and 3 MAGs in each system that were paired by megaBlast were classified as *Firmicutes* (Fig. 3). Mapping of the WGS reads to MAGs indicated that the MAG pairs A27(B63), A9(B41) and A43(B39) were the 1st, 3rd and 4th most abundant *Firmicutes* MAGs in the unamended system and the 2nd, 5th and 1st most abundant *Firmicutes*

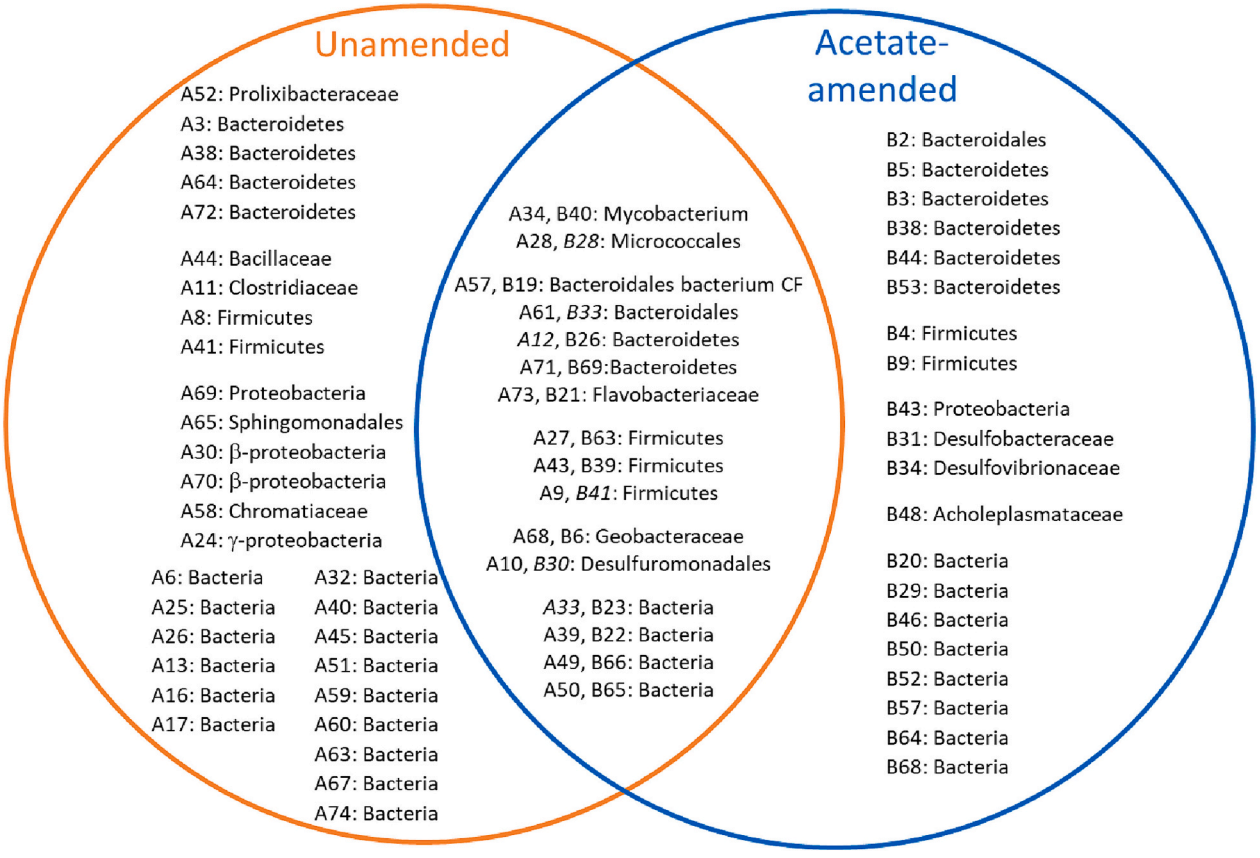

Fig. 3. Venn diagram showing the MAGs in the unamended and acetate-amended microcosms that were > 90 % complete throughout assembly, binning, and reassembly steps from the metaWRAP pipeline. Matching of MAGs in the two systems is based on megaBlast alignment. MAGs shown in italics were < 90 % complete but included due to match with a MAG from the other system.

MAGs in the acetate-amended system, and in each case the relative abundance was larger in the unamended system. The 16S rRNA gene analysis suggests a smaller difference between the systems, but the relative abundance of *Firmicutes* reads was still larger in the unamended than the acetate-amended systems (21 % and 16 % of reads).

3.5. Metabolic potential for metal resistance

Genes coding for resistance to the metal(loid)s As, Cu, Zn, Cd, Cr, were widely detected in MAGs in both systems (SI Table S10 and S11). The ars genes which are thought to code for resistance to arsenicals and antimonials were found in >86 % of high-completeness MAGs in each system. Arsenic has been reported in the ground water at this site presumably arising from some historic industrial process. Similarly, >47 % of these MAGs have cop genes that are thought to have a role in Cu regulation. >38 % of these MAGs have cus genes that are thought to have a role in resistance to Cu and Ag. >56 % of these MAGs have copies of czc genes that encode for Co-Zn-Cd resistance. Interestingly only just over a quarter of the high completeness MAGs in each system had chr genes that confer chromate resistance. The high frequency of metal(loid) resistance genes in MAGs of both systems emphasizes the importance of metal resistance in chromate contaminated systems.

FeGenie found putative iron storage and iron regulation genes in essentially all the high-completeness MAGs in both systems (the only exception was a single MAG that was 92 % complete from the unamended system; SI Table S10 and S11). Similarly, putative Fe(II)/Fe (III) transport and siderophore transport genes were found in most high-completeness MAGs from both systems (84 % and 84 % of MAGs in the unamended system and 87 % and 90 % of MAGs in the acetate-amended system, respectively). This widespread potential for iron transport is to be expected as iron is a necessary micronutrient for most life (Garber et al., 2020). However, only 16 % and 6 % of the high-completeness MAGs in the unamended and acetate-amended systems possessed putative/probable iron reduction genes and 9 % and 6 %, possessed putative siderophore synthesis genes (SI Table S10 and S11).

3.6. Inferred capability for degradation of organic matter

Minpath (Ye and Doak, 2009) was used to search the MAGs for various KEGG pathways associated with the degradation of organic compounds produced by hydrolysis of complex organic matter. This analysis suggests that the metabolic capability to oxidise carbohydrates, amino acids and aromatic compounds is widespread in both systems, with similar proportions of the MAGs able to oxidise these substrates (Table 1). However, 18 % of MAGs in the unamended system have the metabolic capability to metabolise fatty acids, whereas just 9 % of MAGs in the acetate-amended system have this capability. Further, if the proportion of the WGS reads in each system that map onto each MAG is taken as a guide to relative abundance then the relative abundance of bacteria capable of oxidising fatty acids was 4× larger in the unamended system than in the acetate amended system. This is largely due to the difference in relative abundance of the MAG pair A73(B21) (32 % vs 2 % of reads), which were classified to the family *Flavobacteriaceae* (in the phylum *Bacteroidetes*).

3.7. Sulfur reduction is a key process in both systems

The geochemical data shows that the two systems had progressed past reduction of nitrate and nitrite as electron acceptors, to the point where sulfur reduction was just beginning in unamended system and was well advanced in the acetate amended system. Fig. 4 shows the pathways of S assimilation and dissimilatory metabolism. The first step, formation of Adenosine 5'-Phosphosulfate (APS) is common to both assimilatory and dissimilatory pathways and requires energy from ATP hydrolysis (Grein et al., 2013). In the dissimilatory pathway APS is then reduced to sulfite and sulfide by the cytoplasmic enzymes AprAB and

Table 1
Proportion of MAGs that are MinPath positive for the glycolysis, fatty acid degradation, amino acid degradation and benzoate degradation pathways, and the percentage of reads from each population that are associated with those MAGs.

Pathway		Unamended system		Acetate-amended system	
		% of MAGs	% of reads	% of MAGs	% of reads
Glycolysis (ko00010)	Carbohydrate metabolism	48 %	18 %	41 %	12 %
Fatty acid degradation (ko00071)	Lipid metabolism	18 %	47 %	9 %	11 %
Valine, leucine and isoleucine degradation (ko00280)	Amino acid metabolism	7 %	2 %	6 %	1 %
tyrosine degradation (ko00350)	Amino acid metabolism	55 %	51 %	53 %	21 %
phenylalanine degradation (ko00360)	Amino acid metabolism	84 %	69 %	84 %	60 %
tryptophan degradation (ko00380)	Amino acid metabolism	23 %	7 %	22 %	8 %
Benzoate degradation (ko00362)	Xenobiotics biodegradation and metabolism	61 %	24 %	56 %	48 %

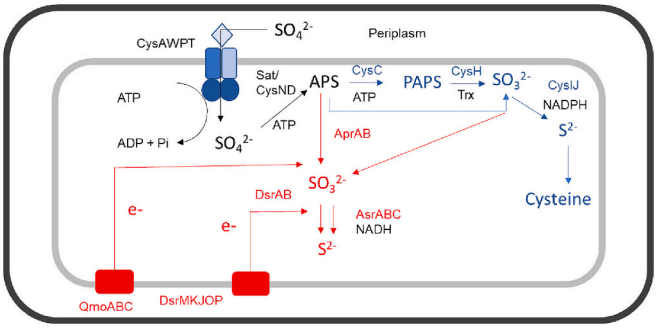

Fig. 4. Pathways of sulfur metabolism in bacteria. Blue; pathway of sulfur assimilatory metabolism. Red; pathway of sulfur dissimilatory metabolism. CysAWPT ABC transporter for sulfate uptake from the periplasm. Sat/CysND activates sulfate for metabolism by either pathway. CysC, CysH, CysIJ genes of assimilatory metabolism. Trx, thioredoxin. AprAB and DsrAB genes of dissimilatory sulfate metabolism. Electrons for the reduction come from QmoABC and DsrMKJOP respectively, linking to quinone reoxidation as part of electron transport. AsrABC genes of anaerobic sulfite reduction. NAD(*P*)H; Nicotinamide adenine dinucleotide (phosphate) reduced form. Sulfide can exit the cell as membrane permeable hydrogen sulfide (H_2S).

DsrAB (Odom and Peck, 1981). Electrons for this reaction are provided by membrane proteins QmoABC and DsrMKJOP (Grein et al., 2013). Some bacteria also contain a pathway for anaerobic sulfite reduction (AnSR) mediated by genes AsrABC (Huang and Barrett, 1991) with electrons for the reduction coming from NADH (Fig. 4). The product of both DSR and AnSR is sulfide which as H_2S is membrane permeable and can be released from the cell.

The presence or absence of genes for these pathways was determined as described in materials and methods and the MAGs which contained a more complete set of genes than would occur by chance are shown in Table 2. The AnSR pathway is present in similar numbers of MAGs in the unamended (8) and acetate amended systems (7) but the relative abundance of those MAGs is much higher in the acetate amended system; 22.7 % vs 4.0 % (Table 2). The MAG B6, which is the most abundant

Table 2
Relative abundance of MAGs in the unamended system and the acetate-amended system that contain a significant proportion of genes for dissimilatory sulfate reduction (DSR) or anaerobic sulfite reduction (AnSR).

System	MAG	Rel. abundance of MAG in the system	Fisher test positive	
			AnSR	DSR
Unamended	A4	0.5 %	✓	
	A8	0.7 %	✓	
	A11	0.5 %	✓	
	A14	0.4 %	✓	
	A26	0.4 %	✓	
	A53	0.2 %	✓	
	A67	0.3 %	✓	
	A68[a]	1.1 %	✓	
	A70	5.0 %		✓
Rel. abundance of MAGs containing pathway			4.0 %	5.0 %
Acetate-amended	B6[a]	18.0 %	✓	
	B7	0.2 %		✓
	B20	0.8 %	✓	
	B24	0.4 %	✓	
	B29	11.3 %		✓
	B31	0.5 %	✓	✓
	B34	2.2 %	✓	✓
	B58	0.2 %		✓
	B59	0.2 %	✓	✓
	B68	0.5 %	✓	✓
Rel. abundance of MAGs containing pathway			22.7 %	15.1 %

[a] MegaBLAST indicates that A68 and B6 are a pair of very similar MAGs.

MAG in the acetate amended system, is the main contributor to this difference. It is paired with MAG A68, the most abundant of the 8 MAGs in the unamended system that are positive for AnSR, but its relative abundance (18.8 %) is far higher than that of A68 (1.1 %). The DSR pathway was present in seven MAGs in the acetate-amended system but only one MAG in the unamended system, and the relative abundance of those MAGs is much higher in the acetate-amended system; 15.1 % vs 5.0 % (Table 2). Several MAGs in the acetate amended system have both the DSR pathway and AnSR pathways whereas other MAGs have one or the other.

Fig. 5 displays this information as a heat map for all the MAGs in each system which were positive for KEGG pathway ko00920 (sulfur metabolism). The dendrograms on the figure represent unsupervised hierarchical clustering based on similar/dissimilar patterns of relative abundance from each gene set (columns) per MAG (rows) (see methods for more details). Clustering therefore supports the idea that genes are present or absent together. For the purposes of this figure anaerobic sulfite reduction, indicated by the presence of asr[ABC], has been classified as a dissimilatory-type pathway. The genes Sat and CysNC are classified as belonging to both as they produce sulfite that is a substrate for either CysIJ in the assimilatory pathway or DsrAB/AsrABC for energy metabolism (Fig. 4). At the top of the figure are a group of MAGs which have the genes for the assimilatory pathway but neither the classical dissimilatory sulfate reduction pathway nor anaerobic sulfite reduction. These are found in both acetate amended and unamended systems and across MAGs classified to the phyla *Bacteroidetes* and *Proteobacteria*. A cluster of MAGs noted previously (Table 2) contain the genes apr[AB12] and ds[rv][AB] indicating the presence of the dissimilatory sulfate reduction pathway and correspond to the phyla *Proteobacteria* and *Firmicutes*. These are found predominantly in the acetate amended system and many of these MAGs have asr[ABC] as well, indicating they also have capacity for anaerobic sulfite reduction. At the bottom of the heat map is a large number of MAGs which have asr[ABC] either alone (where it presumably reduces sulfite taken up from the environment) or together with the genes required to produce sulfite intracellularly. Many of these MAGs are taxonomically unclassified.

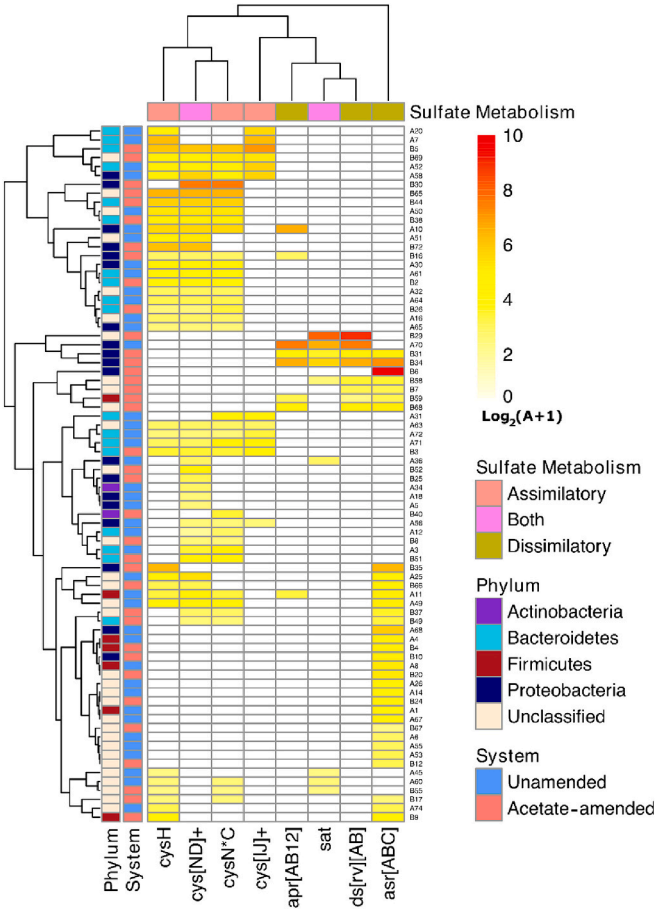

Fig. 5. Heat map showing the distribution and relative abundance of genes for assimilatory sulfate metabolism and dissimilatory sulfate metabolism (ASR and DSR pathways). All MAGs containing sulfate metabolism-assigned genes (ko00920) were selected for the heat map plot regardless of their statistical significance from the Fisher Exact Test performed for assessing either DSR or AnSR pathway enrichment. Relative abundance of each gene set (columns) per MAG (rows) is represented by $Log_2(A + 1)$, where abundance (A) is equal to the number of gene copies in the set per MAG multiplied by the MAG's GCPM (genome copies per million reads) calculated through the "quant_bins" module from the metaWRAP pipeline. A hierarchical clustering relying on $Log_2(A + 1)$ values was performed for both rows and columns. For the purpose of this figure, anaerobic sulfide reduction has been classed as a DSR pathway.

In order to visually compare the most abundant MAGs in each system which were positive for KEGG pathway ko00920, the genetic loci, relative abundance, and amino acid sequence conservation were displayed on a circosPlot (Fig. 6) using the same quantification metric as for the heat map in Fig. 5, plus tBlastX pairwise alignment results. Linking lines and ribbons in the middle of the circle correspond to genomic stretches with significant amino acid conservation (length $\geq$ 30 aa, identity $\geq$50 %, e-value $<1e^{-3}$). These lines and ribbons therefore highlight potential evolutionary relationships between different MAGs from either the same or different systems. A7 and A70 were the only MAGs among the six most abundant in the unamended system which were ko00920 positive, whereas five of the six most abundant MAGs in the acetate amended system B6, B29, B30, B35 and B65 were positive. A68 was added to the chart as the most abundant AnSR-positive MAG in system A (Table 2), and identified as closely related to B6 by the previous megaBlast analysis. A high-level of amino acid sequence conservation between MAGs A68 and B6 (both classified as *Geobacteraceae*) indicates a potential evolutionarily close relationship with a high synteny degree (Fig. 6). However, B6 is much more abundant in system B than A68 is in system A (Table 2). Multiple connections between non-

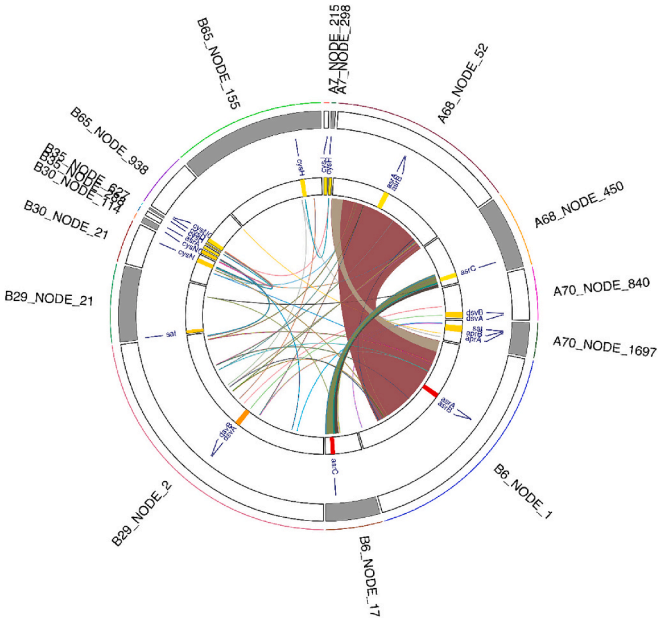

Fig. 6. CircosPlot of the most abundant MAGs that contain genes assigned to the sulfur metabolism KEGG pathway (ko00920). White and grey rectangles represent MAG's contigs (or NODEs) from the metaWRAP "reassemble_bins" module and their respective sizes (in bp). Sequence B29_NODE_2 being the longest (220,620 bp) and sequence B35_NODE_627 the shortest (970 bp). Sulfur metabolism gene loci are displayed along with their respective relative abundance (same $Log_2(A + 1)$ yellow-red colour scale from Fig. 5). Linking lines in the middle of the circle correspond to amino acid conservation from a tBlastX analysis (e-value $<1e^{-3}$, length $\geq$ 30 aa, and identity $\geq$50 %). Ribbons depict larger conserved genomic regions (>2 kb) from the same tBlastX results, indicating a potentially high degree of synteny. Different line colours are merely for the sake of better visualisation.

sulfur gene loci suggest that there are additional genetic similarities between MAGs in these regions which may or may not relate to sulfate metabolism. It is also clear from the plot that gene order is not strongly conserved between distantly related MAGs.

4. Discussion

4.1. Iron reduction was not the dominant respiratory process in either system

The soil used to establish the microcosms was recovered from a former topsoil layer that was beneath a COPR tip and contained about ~3 % organic carbon and a diverse bacterial population. Prior to recovery it was below the perched water table in the waste heap and, as a result, this soil was anaerobic and essentially all the microbially available iron was in the reduced Fe(II) oxidation state. Aqueous Cr(VI) in the water used to make the microcosms was very quickly removed from solution at the start of the microcosm experiments, most probably by reductive precipitation as Cr(III) by Fe(II) oxidation to Fe(III) (Buerge and Hug, 1999), but without much decrease in the proportion of the microbially available iron present as Fe(II) as it was available in excess. Subsequent Cr(VI) spikes were similarly removed very quickly.

However, given that a very high proportion of the "microbially available" Fe was in the reduced Fe(II) oxidation state in both the original soil and subsequently through both microcosm series, it is interesting that putative iron reduction and probable iron reduction genes were found in only 16 % and 6 % of the high-completeness MAGs in the unamended and acetate-amended systems. Similarly, putative siderophore synthesis genes were found in 9 % and 6 % of high-completeness MAGs in the unamended and acetate-amended systems. This may reflect that the samples for metagenomic analysis were taken at a point when sulfate removal from solution (a marker for sulfate reduction) had just started in the unamended system, and sulfate removal was well underway in the acetate-amended system (Fig. 2(d)). Dissolved sulfide can react quickly with poorly crystalline Fe(III)-(oxy) hydroxides when 5 < pH < 9 to produce elemental sulfur, and reduced Fe(II) (Canfield et al., 1992; Peiffer et al., 1992; Poulton et al., 2004). Dissolved sulfide can also react with Cr(VI) to produce elemental sulfur and Cr(III) hydroxides although the reaction is very slow above pH 8 (Kim et al., 2001). So, once dissimilatory sulfate reduction had become established, microbial iron reduction is unnecessary to maintain the high proportion of the "microbially available" iron as Fe(II) even when the system is spiked with Cr(VI).

4.2. The importance of sulfate and sulfite reduction in the acetate-amended system

Both DSR and AnSR genes were overrepresented in the acetate amended system compared to the unamended system, which is most likely a reflection that sulfur reduction was better established in the acetate amended system. The classified MAGs which contained AnSR or DSR genes were from the phyla *Proteobacteria* and *Firmicutes* (Fig. 5). Bacteria carrying the dsrAB gene have previously been shown to cluster in the phyla *Proteobacteria*, *Firmicutes*, and *Actinobacteria*, with the largest group within the *δ-proteobacteria* (Müller et al., 2015; Wolf et al., 2022). In contrast bacteria carrying the asrABC genes are spread widely among five phyla *Actinobacteria*, *Bacteroidetes, Firmicutes*, *Fusobacteria* and *Spirochaetes*. It has been proposed that this pathway is more readily transferred by lateral gene transfer, whereas lateral gene transfer of dsrAB is not common (Wolf et al., 2022).

Four MAGs in the acetate amended system carried genes for both AnSR and DSR (B34, B31, B68 and B59, in order of relative abundance; Table 2, Fig. 5). Whether both activities are expressed under these conditions is not known but the dual genetic capability to perform AnSR and DSR appears more widespread than generally appreciated. Interestingly, MAGs B31 and B34 (like B6 mentioned above) are *δ-proteobacteria*. Search of the UniProt database (accessed 6–9-23) reveals 17 hits for asrA within the δ-proteobacteria, but with the exception of one hit, *Geobacter sulfurreducens* (Inoue et al., 2018), these were from unassembled whole-genome shotgun sequencing. This suggests that δ-proteobacteria can be added to the list of phyla that have AnSR capability.

The 16S rRNA gene sequence analysis indicates that the conditions in the acetate amended microcosms favoured *δ-proteobacteria*. The MAG relative abundance data indicates that the imbalance is largely due to the sulfate reducing MAGs B6(A68), B34 and B31 which are associated with the orders *Desulfuromonadales*, *Desulfovibrionales* and *Desulfobacterales*, respectively. Interestingly, the 16S rRNA gene analysis shows only a small difference in the relative abundance of *Firmicutes* reads between the two systems. Thus, while acetate addition clearly favours the growth of *δ-proteobacteria* that possess the AnSR and/or DSR pathways, it does not favour *Firmicutes* species that possess the AnSR pathway.

Many *Geobacteraceae*, *Desulfovibrionaceae* and *Desulfobacteraceae* species are sulfate reducing bacetria, and most *Geobacteraceae*, many *Desulfobacteraceae* and some *Desulfovibrionaceae* species can use acetate as an electron donor (Thauer et al., 1989; Sun et al., 2000; Lee et al., 2003; Kuever et al., 2004; Muyzer and Stams, 2008; Röling, 2014). The fact that 6 other MAGs in the acetate amended system that possess either the AnSR pathway, DSR pathway or both, and 4 MAGs in the unamended system that possess the AnSR pathway were taxonomically unclassified (Fig. 5), further demonstrates that this environment has a unique microbial community.

In the unamended system the relative abundance of MAGs carrying AnSR genes was similar to that of MAGs carrying DSR genes, and in the acetate-amended system MAGs carrying AnSR genes were slightly more

abundant (Table 2). In the human gut microbiome, AnSR genes can be twice as abundant as DSR genes (Wolf et al., 2022). Together these studies suggest a potential knowledge gap, as there has been far more research into the DSR pathway than the AnSR pathway. Importantly, studies of sulfate reduction in environmental microbiomes that focus solely on the DSR pathway are likely to misrepresent real environmental systems.

4.3. Metabolic capability for oxidation of organic matter

Oxidation of soil organic matter starts with hydrolysis of complex organic molecules to produce aromatics, long-chain fatty acids, amino acids, and sugar residues, which are oxidised by bacteria to produce CO_2 and short-chain fatty acids, particularly acetate (Lovley, 1991; Gerke, 2018). As a result, acetate is available in anaerobic ecosystems and is used as an electron donor by anaerobic respiratory bacteria and as a substrate for methanogenesis (Thauer et al., 1989; Lee et al., 2003; Muyzer and Stams, 2008; Fotidis et al., 2013; Yoon et al., 2013). Anaerobic bacterial respiration must have been supported solely by electron donors derived from the relic organic matter in the unamended system, whereas plentiful acetate was available in the acetate-amended system. MinPath indicated that the metabolic capability to oxidise carbohydrates, amino acids and aromatic compounds is widespread in both systems, with similar proportions of the MAGs encoding genes with ability to oxidise these substrates. However, the metabolic capability to metabolise fatty acids was more widespread in the unamended system than in the acetate-amended system. This difference probably arose because the bacterial population in the unamended system evolved to metabolise the full range of electron donors originating from the relic organic matter, whereas the acetate-amended system could support a larger population of bacteria that could respire using acetate as an electron donor which anaerobic bacteria usually metabolise via the acetyl-CoA pathway (Schauder et al., 1986) or by a modified citric acid pathway (Brandis-Heep et al., 1983).

Bacteroidetes were a dominant phylum in both the unamended and the acetate amended microcosms. *Bacteroidetes* are linked to the breakdown of SOM and the abundance of *Bacteroidetes* species has been found to be positively correlated with soil organic C mineralisation rates (Fierer et al., 2007). Thus, it is interesting to note that the relative abundance of *Bacteroidetes* species was lower in the acetate-amended system, which was less dependent on SOM for electron donors, than in the unamended system where anaerobic respiration depended solely by electron donors derived from SOM. However, none of the *Bacteriodetes* MAGs in either system contained either the AnSR or DSR pathway even though sulfur reduction was, or was becoming, an important metabolic process in both systems.

As a carbon source, acetate releases less energy during dissimilatory metabolism than sugar residues and longer chain fatty acids, but the yield is still sufficient to support bacterial life (Langmuir, 1997; Scholten et al., 2002; Muyzer and Stams, 2008). As a result, many species have evolved to oxidise acetate during anaerobic respiration using variously nitrate, nitrite, Mn(IV), Fe(III), sulfate and other sulfur species as electron acceptors (Ingvorsen et al., 1984; Thauer et al., 1989; Lovley et al., 1993; Caccavo et al., 1994). The electron acceptors are usually consumed in the stated order, as there is sequentially less available energy from these redox reactions. The addition of acetate as an additional energy source resulted in the acetate-amended microcosms progressing further down the cascade of electron accepting processes than the unamended system. Thus, it should be anticipated that the acetate-amended system supported a larger proportion of bacteria able to use sulfate as an electron acceptor. The greater similarity between the acetate-amended replicates indicated by the 16S rRNA gene analysis suggests that a smaller of range of bacteria in the soil inoculum were well adapted to the conditions that developed in the acetate-amended system than to those in the unamended system.

4.4. Comparison with other alkaline environments

A study of samples from 3 COPR disposal sites in China using 16S rRNA gene sequencing concluded that bacterial diversity was inversely correlated with Cr concentration and that diversity recovered over a 30 year time span (Min et al., 2017). This is observation is consistent with the finding that the microbial community in the initial soil sample from below the COPR waste reported here was quite diverse. The waste was tipped >100 years ago and (a)biotic Fe reduction quickly removed Cr (III) from solution in the subsurface soil layer. Thus, these populations were not exposed to acute Cr toxicity. A major difference is that the populations studied by Min et al. (2017) were surface samples, therefore from an aerobic environment, whereas the samples in the present study were from a depth of 3.4 m and therefore strictly anaerobic. Other anaerobic (alkaline) environments that have been studied using metagenomic methods include soda lake sediments (Vavourakis et al., 2018) and diverse terrestrial, fresh water and marine sediments (Anantharaman et al., 2018; Vigneron et al., 2021). These studies all demonstrate the importance of dissimilatory sulfate metabolism in these anaerobic environments and also the enormous microbial diversity in extreme environments that has not been previously described. Our study has begun to provide insights into the metabolic capabilities of microbial populations at a legacy COPR disposal site which can lead to the development of engineering strategies to harness this potential.

5. Conclusion

The principal pathways to harm to human health from Cr(VI)-containing wastes involve either ingestion or inhalation of the waste, or water contaminated by the waste. Dermal exposure to the waste or contaminated water is also hazardous. This makes environmental remediation of legacy high-lime COPR disposal sites an intractable problem because removal and disposal at a licensed landfill is highly inadvisable, as it will involve large-scale excavation and transport of the waste that will inevitably generate airborne dusts. Capping the waste in-situ with an engineered barrier can eliminate direct contact with the waste, prevent dust generation, and reduce rainwater infiltration into the waste, and thus greatly reduce the risk posed by a COPR tip. However, it is extremely difficult to prevent all water ingress into a waste pile, and thus there is still the potential for the tip to release Cr(VI)-contaminated water to the wider environment.

This work suggest that bacterial processes could be harnessed to create a Cr(VI) trap-zone beneath COPR tips without the need to disturb the waste. If a suitable electron donor is injected via a borehole into the soil beneath a tip, natural soil bacteria without oxygen will respire anaerobically reducing nitrate, Mn(VI), microbially available Fe(III) and sulfate, in turn. As demonstrated in this study, reduction of sulfate and sulfite to produce sulfide can result in Cr(VI) reduction either directly or via Fe(II) formation. As the main steps in the redox cascade are mediated by numerous common soil bacteria, and since sulfate is a common co-contaminant at COPR sites, it should only be necessary to supply a sufficient quantity of a suitable electron donor to ensure that Fe(III) and/or sulfate -reducing conditions develop. This study has shown that a microbial community with this capability exists within in a low permeability soil layer just 0.5 m from the hostile geochemical environment within the COPR waste.

Ethics approval and consent to participate

N/A

Consent for publication

N/A

Funding

This work was supported by the Royal Society [APX\R1\201174].

CRediT authorship contribution statement

Douglas I. Stewart: Conceptualization, Funding acquisition, Investigation, Methodology, Project administration, Validation, Visualization, Writing – original draft. **Elton J.R. Vasconcelos:** Data curation, Formal analysis, Investigation, Software, Visualization, Writing – review & editing. **Ian T. Burke:** Investigation, Methodology, Writing – review & editing. **Alison Baker:** Investigation, Visualization, Writing – original draft.

Declaration of competing interest

The authors declare that they have no known competing financial interests or personal relationships that could have appeared to influence the work reported in this paper.

Data availability

The sequence data and MAGs generated and analysed during the current study are available in the ENA repository: study PRJEB51999. All other data generated or analysed during this study are included in this published article and its supplementary information files.

Acknowledgement

The authors would like to thank the Canals and Rivers Trust for access to the field site. We would also like to thank Ian Carr, Morag Raynor and Carolina Lascelles at the Next Generation Sequencing Facility, Leeds Institute for Biomedical and Clinical Sciences, for their valuable advice and support. All computational data analyses were undertaken on ARC3, part of the High Performance Computing facility at the University of Leeds, UK, to whom we are grateful for their technical assistance. We also received valuable assistance from many other colleagues at the University of Leeds: Fiona Keay and Rachel Gasior (School of Geography) with ion chromatography; Lesley Neve (School of Earth and Environment) for XRD analysis; Felipe Sepulveda (School of Civil Engineering) for loss on ignition analysis; Dave Elliott, Emma Tidswell and Morgan McGowan (School of Civil Engineering) for assistance with the microcosm experiments.

Appendix A. Supplementary data

Software sources, search targets for potential metal resistance and S metabolism genes, further compositional data on the grey clay and ditch water, further geochemical data from the microcosm experiments, alpha and beta diversity between replicate microcosms and between systems based on 16S rRNA gene sequencing, properties of the metagenome-assembled genomes (MAGs) and genetic features in the high completeness (>90 % complete) MAGs. Supplementary data to this article can be found online at https://doi.org/10.1016/j.scitotenv.2024.172507.

References

Albertsen, M., Hugenholtz, P., Skarshewski, A., Nielsen, K.L., Tyson, G.W., Nielsen, P.H., 2013. Genome sequences of rare, uncultured bacteria obtained by differential coverage binning of multiple metagenomes. Nat. Biotechnol. 31 (6), 533–538.

Alderson, M. R., N. S. Rattan and Bidstrup (1981). "Health of workmen in the chromate-producing industry in Britain." Br. J. Ind. Med. 38: 117–124.

Alneberg, J., Bjarnason, B.S., de Bruijn, I., Schirmer, M., Quick, J., Ijaz, U.Z., Lahti, L., Loman, N.J., Andersson, A.F., Quince, C., 2014. Binning metagenomic contigs by coverage and composition. Nat. Methods 11 (11), 1144–1146.

Altschul, S.F., Madden, T.L., Schäffer, A.A., Zhang, J., Zhang, Z., Miller, W., Lipman, D.J., 1997. Gapped BLAST and PSI-BLAST: a new generation of protein database search programs. Nucleic Acids Res. 25 (17), 3389–3402.

Anantharaman, K., Hausmann, B., Jungbluth, S.P., Kantor, R.S., Lavy, A., Warren, L.A., Rappé, M.S., Pester, M., Loy, A., Thomas, B.C., Banfield, J.F., 2018. Expanded diversity of microbial groups that shape the dissimilatory sulfur cycle. ISME J. 12 (7), 1715–1728.

Aoki-Kinoshita, K.F., Kanehisa, M., 2007. Gene annotation and pathway mapping in KEGG. Methods Mol. Biol. 396, 71–91.

Atkins, J., 2009. Modelling Groundwater and Chromite Migration through an Old Spoil Tip in Copley. MSc Dissertation,. University of Leeds.

Babraham_Bioinformatics. (2023a, 01–03-23). "FastQC - A quality control tool for high throughput sequence data.", from https://www.bioinformatics.babraham.ac.uk/projects/fastqc/.

Babraham_Bioinformatics. (2023b, 19–11-19). "Trim Galore - A wrapper tool around Cutadapt and FastQC to consistently apply quality and adapter trimming to FastQ files, with some extra functionality for MspI-digested RRBS-type (Reduced Representation Bisufite-Seq) libraries.", from https://www.bioinformatics.babraham.ac.uk/projects/trim_galore/.

Barnhart, J., 1997. Occurrences, uses, and properties of chromium. Regul. Toxicol. Pharmacol. 26 (1 Pt 2), S3–S7.

Bier, R.L., Wernegreen, J.J., Vilgalys, R.J., Ellis, J.C., Bernhardt, E.S., 2020. Subsidized or stressed? Shifts in freshwater benthic microbial metagenomics along a gradient of alkaline coal mine drainage. Limnol. Oceanogr. 65 (S1), S277–S292.

Brandis-Heep, A., Gebhardt, N.A., Thauer, R.K., Widdel, F., Pfennig, N., 1983. Anaerobic acetate oxidation to CO2 by Desulfobacter postgatei. Arch. Microbiol. 136 (3), 222–229.

Breeze, V.G., 1973. Land reclamation and river pollution problems in Croal Valley caused by waste from chromate manufacture. J. Appl. Ecol. 10 (2), 513–525.

Brito, F., Ascanio, J., Mateo, S., Hernández, C., Araujo, L., Gili, P., Martín-Zarza, P., Domínguez, S., Mederos, A., 1997. Equilibria of chromate(VI) species in acid medium and ab initio studies of these species. Polyhedron 16 (21), 3835–3846.

Buerge, I.J., Hug, S.J., 1999. Influence of mineral surfaces on chromium(VI) reduction by Iron(II). Environ. Sci. Technol. 33 (23), 4285–4291.

Burke, I.T., Boothman, C., Lloyd, J.R., Livens, F.R., Charnock, J.M., McBeth, J.M., Mortimer, R.J.G., Morris, K., 2006. Reoxidation behavior of technetium, iron, and sulfur in estuarine sediments. Environ. Sci. Technol. 40 (11), 3529–3535.

Burke, T., Fagliano, J., Goldoft, M., Hazen, R.E., Iglewicz, R., McKee, T., 1991. Chromite ore processing residue in Hudson County, New Jersey. Environ. Health Perspect. 92, 131–137.

Caccavo, F., Lonergan, D., Lovley, D., Davis, M., Stolz, J., McInerney, M., 1994. Geobacter sulfurreducens sp. nov., a hydrogen- and acetate-oxidizing dissimilatory metal-reducing microorganism. Appl. Environ. Microbiol. 60 (10), 3752–3759.

Canfield, D.E., Raiswell, R., Bottrell, S.H., 1992. The reactivity of sedimentary iron minerals toward sulfide. Am. J. Sci. 292 (9), 659–683.

Cefalu, W., Hu, F., 2004. Role of chromium in human health and in diabetes. Diabetes Care 27 (11), 2741–2751.

Chandra, P., Kulshreshtha, K., 2004. Chromium accumulation and toxicity in aquatic vascular plants. Bot. Rev. 70 (3), 313–327.

Cole, J.R., Wang, Q., Fish, J.A., Chai, B., McGarrell, D.M., Sun, Y., Brown, C.T., Porras-Alfaro, A., Kuske, C.R., Tiedje, J.M., 2014. Ribosomal database project: data and tools for high throughput rRNA analysis. Nucleic Acids Res. 42 (Database issue), D633–D642.

Costa, M., 1997. Toxicity and carcinogenicity of Cr(VI) in animal models and humans. Crit. Rev. Toxicol. 27 (5), 431–442.

Cotta, S.R., Pellegrinetti, T.A., Andreote, A.P.D., Costa, J.S., Sarmento, H., Fiore, M.F., 2022. Disentangling the lifestyle of bacterial communities in tropical soda lakes. Sci. Rep. 12 (1), 7939.

Darrie, G., 2001. Commercial extraction technology and process waste disposal in the manufacture of chromium chemicals from ore. Environ. Geochem. Health 23 (3), 187–193.

Ding, W., Stewart, D.I., Humphreys, P.N., Rout, S.P., Burke, I.T., 2016. Role of an organic carbon-rich soil and Fe(III) reduction in reducing the toxicity and environmental mobility of chromium(VI) at a COPR disposal site. Sci. Total Environ. 541, 1191–1199.

Dröge, J., Gregor, I., McHardy, A.C., 2015. Taxator-tk: precise taxonomic assignment of metagenomes by fast approximation of evolutionary neighborhoods. Bioinformatics 31 (6), 817–824.

Edgar, R.C., 2013. UPARSE: highly accurate OTU sequences from microbial amplicon reads. Nat. Methods 10 (10), 996–998.

ENTEC, 2008. Data on Manufacture, Import, Export, Uses and Releases of Sodium Dichromate as well Information on Potential Alternatives to its Use. EU Framework contract ECHA/2008/2 EU.

Ewels, P., Magnusson, M., Lundin, S., Käller, M., 2016. MultiQC: summarize analysis results for multiple tools and samples in a single report. Bioinformatics 32 (19), 3047–3048.

Fierer, N., Bradford, M.A., Jackson, R.B., 2007. Toward an ecological classification of soil bacteria. Ecology 88 (6), 1354–1364. https://doi.org/10.1890/05-1839.

Fotidis, I.A., Karakashev, D., Kotsopoulos, T.A., Martzopoulos, G.G., Angelidaki, I., 2013. Effect of ammonium and acetate on methanogenic pathway and methanogenic community composition. FEMS Microbiol. Ecol. 83 (1), 38–48.

Garber, A.I., Nealson, K.H., Okamoto, A., McAllister, S.M., Chan, C.S., Barco, R.A., Merino, N., 2020. FeGenie: a comprehensive tool for the identification of Iron genes and Iron gene neighborhoods in genome and metagenome assemblies. Front. Microbiol. 11, 37.

Gerke, J., 2018. Concepts and misconceptions of humic substances as the stable part of soil organic matter: a review. Agronomy 8 (5), 76.

Grein, F., Ramos, A.R., Venceslau, S.S., Pereira, I.A.C., 2013. Unifying concepts in anaerobic respiration: insights from dissimilatory sulfur metabolism. Biochim. Biophys. Acta (BBA) – Bioener. 1827 (2), 145–160.
Hill, M.O., 1973. Diversity and evenness: a unifying notation and its consequences. Ecology 54 (2), 427–432.
Huang, C.J., Barrett, E.L., 1991. Sequence analysis and expression of the salmonella typhimurium asr operon encoding production of hydrogen sulfide from sulfite. J. Bacteriol. 173 (4), 1544–1553.
Ingvorsen, K., Zehnder, A.J., Jørgensen, B.B., 1984. Kinetics of sulfate and acetate uptake by Desulfobacter postgatei. Appl. Environ. Microbiol. 47 (2), 403–408.
Inoue, K., Ogura, Y., Kawano, Y., Hayashi, T., 2018. Complete genome sequence of Geobacter sulfurreducens strain YM18, isolated from river sediment in Japan. Genome Announc. 6 (19) https://doi.org/10.1128/genomea.00352-00318.
Jacobs, J. A. and S. M. Testa (2005). Overview of Chromium(VI) in the Environment: Background and History. Chromium(VI) Handbook. J. Guertin, J. A. Jacobs and C. P. Avakian. Boca Raton, Fla., CRC Press.
Jensen, J.L., Christensen, B.T., Schjønning, P., Watts, C.W., Munkholm, L.J., 2018. Converting loss-on-ignition to organic carbon content in arable topsoil: pitfalls and proposed procedure. Eur. J. Soil Sci. 69 (4), 604–612.
Kang, D.D., Li, F., Kirton, E., Thomas, A., Egan, R., An, H., Wang, Z., 2019. MetaBAT 2: an adaptive binning algorithm for robust and efficient genome reconstruction from metagenome assemblies. PeerJ 7, e7359.
Kim, C., Zhou, Q., Deng, B., Thornton, E.C., Xu, H., 2001. Chromium(VI) reduction by hydrogen sulfide in aqueous media: stoichiometry and kinetics. Environ. Sci. Technol. 35 (11), 2219–2225.
Kolde, R., 2019. "pheatmap: Pretty Heatmaps." Retrieved Aug 2023, 2023, from. https://CRAN.R-project.org/package=pheatmap.
Kondo, K., Takahashi, Y., Ishikawa, S., Uchihara, H., Hirose, Y., Yoshizawa, K., Tsuyuguchi, M., Takizawa, H., Miyoshi, T., Sakiyama, S., Monden, Y., 2003. Microscopic analysis of chromium accumulation in the bronchi and lung of chromate workers. Cancer 98 (11), 2420–2429.
Kuever, J., Rainey, F.A., Widdel, F., 2004. Desulfovibrionaceae. Bergey's Manual of Systematics of Archaea and Bacteria 926–938.
Langmuir, D., 1997. Aqueous Environmental Geochemistry. Prentice-Hall.
Lee, J., Phung, N.T., Chang, I.S., Kim, B.H., Sung, H.C., 2003. Use of acetate for enrichment of electrochemically active microorganisms and their 16S rDNA analyses. FEMS Microbiol. Lett. 223 (2), 185–191.
Léonard, A., Lauwerys, R.R., 1980. Carcinogenicity and mutagenicity of chromium. Mutat. Res./Review. Gene. Toxicol. 76 (3), 227–239.
Li, W., Li, X., 2021. Metagenome-assembled genomes infer potential microbial metabolism in alkaline sulphidic tailings. Environ. Microb. 16 (1), 9.
Lovley, D., Giovannoni, S., White, D., Champine, J., Phillips, E., Gorby, Y., Goodwin, S., 1993. Geobacter metallireducens gen. Nov. sp. nov., a microorganism capable of coupling the complete oxidation of organic compounds to the reduction of iron and other metals. Arch. Microbiol. 159, 336–344.
Lovley, D.R., 1991. Dissimilatory Fe(III) and Mn(IV) reduction. Microbiol. Rev. 55 (2), 259–287.
Lovley, D.R., 1993. Dissimilatory metal reduction. Ann. Rev. Microbiol. 47, 263–290.
Lovley, D.R., Phillips, E.J.P., 1986. Availability of ferric iron for microbial reduction in bottom sediments of the freshwater tidal Potomac River. Appl. Environ. Microbiol. 52 (4), 751–757.
Lukaski, H., 1999. CHROMIUM AS A SUPPLEMENT. Annu. Rev. Nutr. 19 (1), 279–302.
Min, X., Wang, Y., Chai, L., Yang, Z., Liao, Q., 2017. High-resolution analyses reveal structural diversity patterns of microbial communities in chromite ore processing residue (COPR) contaminated soils. Chemosphere 183, 266–276.
Müller, A.L., Kjeldsen, K.U., Rattei, T., Pester, M., Loy, A., 2015. Phylogenetic and environmental diversity of DsrAB-type dissimilatory (bi)sulfite reductases. ISME J. 9 (5), 1152–1165.
Muyzer, G., Stams, A.J.M., 2008. The ecology and biotechnology of sulphate-reducing bacteria. Nat. Rev. Microbiol. 6 (6), 441–454.
Nurk, S., Meleshko, D., Korobeynikov, A., Pevzner, P.A., 2017. metaSPAdes: a new versatile metagenomic assembler. Genome Res. 27 (5), 824–834.
Odom, J.M., Peck, H.D., 1981. Localization of dehydrogenases, reductases, and electron transfer components in the sulfate-reducing bacterium Desulfovibrio gigas. J. Bacteriol. 147 (1), 161–169.
Parks, D.H., Imelfort, M., Skennerton, C.T., Hugenholtz, P., Tyson, G.W., 2015. CheckM: assessing the quality of microbial genomes recovered from isolates, single cells, and metagenomes. Genome Res. 25 (7), 1043–1055.
Peiffer, S., Dos Santos Afonso, M., Wehrli, B., Gaechter, R., 1992. Kinetics and mechanism of the reaction of hydrogen sulfide with lepidocrocite. Environ. Sci. Technol. 26 (12), 2408–2413.
Poulton, S.W., Krom, M.D., Raiswell, R., 2004. A revised scheme for the reactivity of iron (oxyhydr)oxide minerals towards dissolved sulfide. Geochim. Cosmochim. Acta 68 (18), 3703–3715.
Pourbaix, M., 1966. Atlas of Electrochemical Equilibria in Aqueous Solutions. Pergamon Press.
Prjibelski, A., Antipov, D., Meleshko, D., Lapidus, A., Korobeynikov, A., 2020. Using SPAdes De Novo Assembler. Curr. Protoc. Bioinformatics 70 (1), e102.
Röling, W.F.M., 2014. The family Geobacteraceae. In: Rosenberg, E., DeLong, E.F., Lory, S., Stackebrandt, E., Thompson, F. (Eds.), The Prokaryotes: Deltaproteobacteria and Epsilonproteobacteria. Berlin, Heidelberg, Springer Berlin, Heidelberg, pp. 157–172.
Schauder, R., Eikmanns, B., Thauer, R.K., Widdel, F., Fuchs, G., 1986. Acetate oxidation to CO2 in anaerobic bacteria via a novel pathway not involving reactions of the citric acid cycle. Arch. Microbiol. 145 (2), 162–172.
Scholten, J.C.M., van Bodegom, P.M., Vogelaar, J., van Ittersum, A., Hordijk, K., Roelofsen, W., Stams, A.J.M., 2002. Effect of sulfate and nitrate on acetate conversion by anaerobic microorganisms in a freshwater sediment. FEMS Microbiol. Ecol. 42 (3), 375–385.
Seemann, T., 2014. Prokka: rapid prokaryotic genome annotation. Bioinformatics 30 (14), 2068–2069.
Shanker, A., Cervantes, C., Loza-Tavera, H., Avudainayagam, S., 2005. Chromium toxicity in plants. Environ. Int. 31 (5), 739–753.
SilentGene. (2019, 7th May 2019). "prokka2kegg python script." from https://github.com/SilentGene/Bio-py/tree/master/prokka2kegg.
Stewart, D.I., Burke, I.T., Mortimer, R.J.G., 2007. Stimulation of microbially mediated chromate reduction in alkaline soil-water systems. Geomicrobiol J. 24, 655–669.
Stewart, D.I., Burke, I.T., Hughes-Berry, D.V., Whittleston, R.A., 2010. Microbially mediated chromate reduction in soil contaminated by highly alkaline leachate from chromium containing waste. Ecol. Eng. 36, 211–221.
Sun, B., Cole, J.R., Sanford, R.A., Tiedje, J.M., 2000. Isolation and characterization of Desulfovibrio dechloracetivorans sp. nov., a marine dechlorinating bacterium growing by coupling the oxidation of acetate to the reductive dechlorination of 2-chlorophenol. Appl. Environ. Microbiol. 66 (6), 2408–2413.
SWRCB, 2022. Proposed Hexavalent Chromium MCL Staff Report. California, California State Water Resources Control Board.
Thauer, R.K., Möller-Zinkhan, D., Spormann, A.M., 1989. Biochemistry of acetate catabolism in anaerobic chemotrophic bacteria. Ann. Rev. Microbiol. 43, 43–67.
Uritskiy, G.V., DiRuggiero, J., Taylor, J., 2018. MetaWRAP-a flexible pipeline for genome-resolved metagenomic data analysis. Microbiome 6 (1), 158.
US-EPA, 1992. "SW-846 Manual: Method 7196a. Chromium hexavalent (colorimetric)." Retrieved 6th Jan 2006.
Vavourakis, C.D., Andrei, A.-S., Mehrshad, M., Ghai, R., Sorokin, D.Y., Muyzer, G., 2018. A metagenomics roadmap to the uncultured genome diversity in hypersaline soda lake sediments. Microbiome 6 (1), 168.
Vigneron, A., Cruaud, P., Culley, A.I., Couture, R.-M., Lovejoy, C., Vincent, W.F., 2021. Genomic evidence for sulfur intermediates as new biogeochemical hubs in a model aquatic microbial ecosystem. Microbiome 9 (1), 46.
Vincent, J.B., 2000. The biochemistry of chromium. J. Nutr. 130 (4), 715–718.
Weber, K.A., Picardal, F.W., Roden, E.E., 2001. Microbially catalyzed nitrate-dependent oxidation of biogenic solid-phase Fe(II) compounds. Environ. Sci. Technol. 35, 1644–1650.
Whittleston, R.A., Stewart, D.I., Mortimer, R.J.G., Ashley, D.J., Burke, I.T., 2011a. Effect of microbially induced anoxia on Cr(VI) mobility at a site contaminated with hyperalkaline residue from chromite ore processing. Geomicrobiol J. 28, 68–82.
Whittleston, R.A., Stewart, D.I., Mortimer, R.J.G., Tilt, Z.C., Brown, A.P., Geraki, K., Burke, I.T., 2011b. Chromate reduction in Fe(II)-containing soil affected by hyperalkaline leachate from chromite ore processing residue. J. Hazard. Mater. 194, 15–23.
WHO, 2020. Chromium in Drinking-Water Background Document for Development of WHO Guidelines for Drinking-Water Quality. World Health Organization, Geneva.
Wolf, P.G., Cowley, E.S., Breister, A., Matatov, S., Lucio, L., Polak, P., Ridlon, J.M., Gaskins, H.R., Anantharaman, K., 2022. Diversity and distribution of sulfur metabolic genes in the human gut microbiome and their association with colorectal cancer. Microbiome 10 (1), 64.
Wu, Y.W., Simmons, B.A., Singer, S.W., 2016. MaxBin 2.0: an automated binning algorithm to recover genomes from multiple metagenomic datasets. Bioinformatics 32 (4), 605–607.
Yang, L., Chen, J., 2022. A comprehensive evaluation of microbial differential abundance analysis methods: current status and potential solutions. Microbiome 10 (1), 130.
Ye, Y., Doak, T.G., 2009. A parsimony approach to biological pathway reconstruction/inference for genomes and metagenomes. PLoS Comput. Biol. 5 (8), e1000465.
Yoon, S., Sanford, R.A., Löffler, F.E., 2013. Shewanella spp. use acetate as an electron donor for denitrification but not ferric iron or fumarate reduction. Appl. Environ. Microbiol. 79 (8), 2818–2822.
Zhang, H., Meltzer, P., Davis, S., 2013. RCircos: an R package for Circos 2D track plots. BMC Bioinform. 14 (1), 244.